R. ULEWICZ, P. TOMSKI

THE EFFECT OF HIGH-FREQUENCIES LOADING ON THE FATIGUE CRACKING OF NODULAR CAST IRON

The article presents the results of fatigue tests using high-frequency loading of nodular cast iron. Nodular cast iron GJS-500-7, GJS-600-3 and cast iron ADI with a tensile strength of R_m = 1 125 MPa were used for the tests. The fatigue tests were conducted on a resonance testing machine. For the cast iron grades under investigation, fatigue characteristics in high and ultra-high-cycle regions were experimentally determined. After the completion of the tests, the fractographic analysis of fatigue fractures was made with the aim of determining the fatigue crack initiation location and the fracture mechanism.

Key words: nodular cast iron, fatigue failure, high frequency fatigue testing, fractography

INTRODUCTION

The fatigue of materials is a continuous process of accumulation of failures forming over a sufficiently long time during operation under the influence of variable mechanical stresses that cause the nucleation and propagation of a crack, which results in the failure of the material and the structure [1]. The accumulation of stresses causes changes in the mechanical properties of the material due to cyclic micro-plastic deformation. At the moment of local stresses reaching a maximal value, the destruction of interatomic bonds occurs during the initiation of micro-cracks, leading to a failure of the structure [2,3]. The fatigue damage of structural materials is the most frequent cause of the threshold state of materials. The fatigue properties of structural materials have been investigated for more than 150 years. The S–N curve (also known as Wöhler curve), including the fatigue limit (referred to N = $2{\times}10^6$–10^7 cycles), has been known since 1858. According to the applicable standards, fatigue data (S–N curves) are generally investigated up to N = 10^7 cycles of loading (steel and cast iron) [4]. Increasing the fatigue strength is gaining importance in solving the general problem of the operational reliability of contemporary machinery, equipment and structures. The analysis of the causes of the failures of machines and structures shows machines and structures shows that about 90 %) of all cracking instances are caused by the fatigue process. Periodically variable stresses, which are much lower than the ultimate strength, as well as the sufficient number of cycles, cause fatigue cracking [5,6]. The contemporary trends towards reducing the wear of materials in machine constructions require their loading level to be in-

creased and their service life extended, which is tantamount to increasing the number of cycles (many times above the conventional limit of 10^7 cycles). This could be accomplished by using high-strength, so generally more brittle and fatigue-prone, materials. These facts encourage one to undertake fatigue lifetime investigation in the very high-cycle (VHC) region ($10^7 < N < 10^{10}$ cycles). The fatigue initiation mechanism in the high-cycle (HC) and VHC regions is a topic of increasing importance, due to increasing demands imposed on the lifetime of engineering components. In this study, the fatigue lifetime of GJS-500-7, GJS-600-3 and ADI in the ultra-wide lifetime region was investigated. The aim was to determine experimentally the fatigue lifetime, and to analyze the fatigue crack initiation.

MATERIAL AND EXPERIMENTAL METHODS

Ferritic-pearlitic matrix cast iron (GJS-500-7), pearlitic-ferritic matrix cast iron (GJS-600-3) and ADI cast iron were qualified for testing. The ADI cast iron was produced through the isothermal treatment of GJS-500-7 cast iron. The treatment parameters were as follows:

- austenitizing at a temperature of 910 ºC for a duration of 30 min.,
- isothermal process at a temperature of 400 ºC for a duration of 60 min.

The mechanical properties of the materials tested are given in Table 1. The microstructure of the ADI cast iron is shown in Figure 1.

Table 1 **Mechanical properties**

Mat.	*Rm* / MPa	HB	*KCU2* / %	*Z* / %
GSJ-500-7	553	171	13,28	10,9
GSJ-600-3	668	198	6,67	7,7
ADI	1 125	280	20,41	9,7

_____

R. Ulewicz, P. Tomski, Czestochowa University of Technology, Czestochowa, Poland

Figure 1 Microstructure of the cast iron (ADI), magn. 400x

The fatigue tests were carried out on a KAUP-ŽU resonance testing machine following the procedure described in reference [7]. The specimen used in fatigue tests using high loading frequencies is shown in Figure 2.
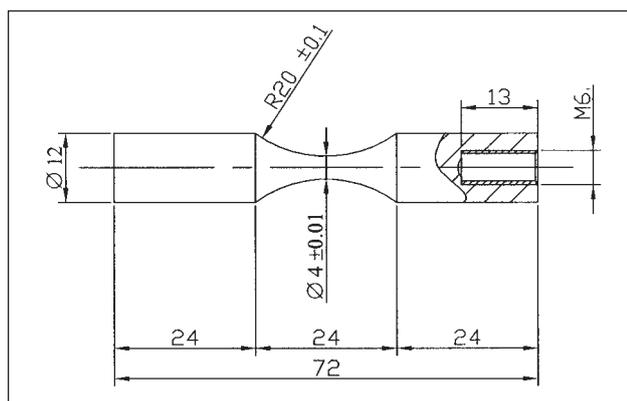

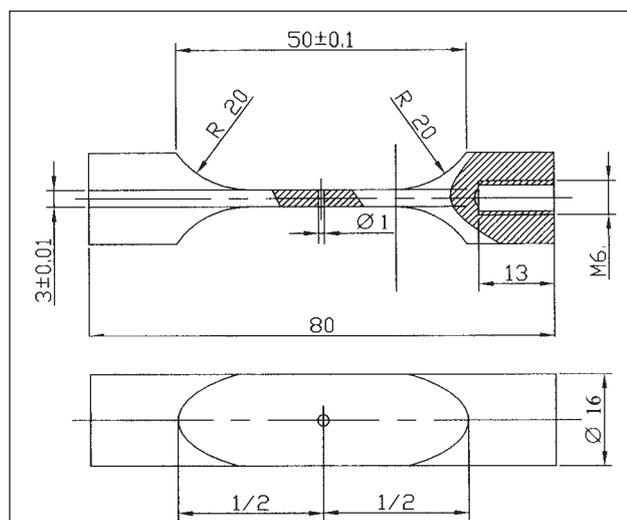**Figure 2** The shape and size of the specimens used in the fatigue test using a high frequency of loading f ≈ 20kHz

Figure 3 The shape and size of the specimen used for the determination of the crack propagation rate at a high frequency of loading f ≈ 20kHz

For the determination of crack propagation rate, the specimen shown in Figure 3 is used. Its shape and size is described in works [7,8].

For the fractographic analysis, a VEGA 3 SB scanning electron microscope (SEM) was used. For each series of specimens, the analysis of fatigue fractures was made. For fatigue crack trajectory testing, ferritic-pearlitic cast iron (GJS-500-7) and pearlitic-ferritic cast iron (GJS-600-3) were chosen. The tests were conducted by loading the specimen with a high frequency of loading f ≈ 20 kHz, at a temperature of T = 20 ± 10°C, R = - 1, whereas the specimen was immersed in methylalcohol as a cooling medium. The examination of the fatigue crack trajectory was made on a Neophot 32 optical microscope and a scanning microscope.

RESULT AND DISCUSSION

The results of the ultra-high-cycle fatigue tests carried out on the KAUP-ŽU high-frequency fatigue testing machine are presented in Figure 4.

The fatigue characteristic curves, the relationships $\sigma_a = f(N_f)$ in the region of $N_f = 6\times10^6$ ¸ 1×10^{10} cycles, were determined with high-frequency loading failure. In all of the three nodular cast iron types, a fatigue fracture occurred within the assumed interval of cycles with decreasing amplitude σ_a and the number of cycles N_f increasing up to the fraction.

For nodular cast iron GJS-500-7, the magnitude of the stress amplitude at $N_f = 5,934\times10^6$ cycles amounted to $\sigma_a = 276$ MPa, while at $N_f = 1,0\times10^{10}$ **cycles,** $\sigma_a = 180$ MPa. For nodular cast iron GJS-600-3, the stress amplitude magnitude at $N_f = 5,371\times10^6$ cycles was $\sigma_a = $ **440** MPa, while at $N_f = 1,0\times10^{10}$, $\sigma_a = 162$ MPa. For nodular cast iron ADI, the stress amplitude magnitude at $N_f = 4,3\times10^7$ cycles was $\sigma_a = 190$ MPa, while at $N_f = 1,0\times10^{10}$ **cycles,** $\sigma_a = 175$ MPa. The least difference in stress amplitude at comparable loading cycles occurred in cast iron ADI. For the ADI cast iron, the least dispersed results were obtained for a given stress amplitude value and a given number of cycles. For the GJS-500-7 cast iron, the dispersion was greater, while the
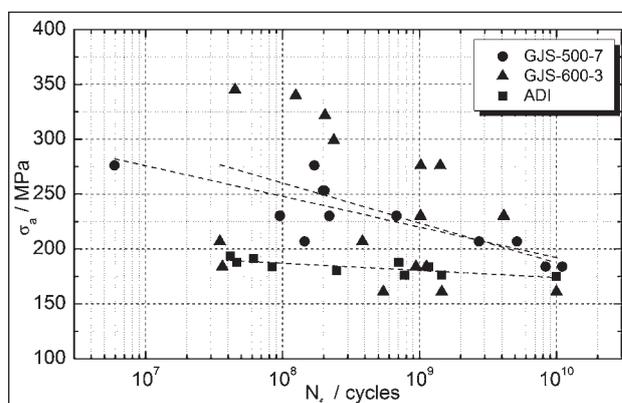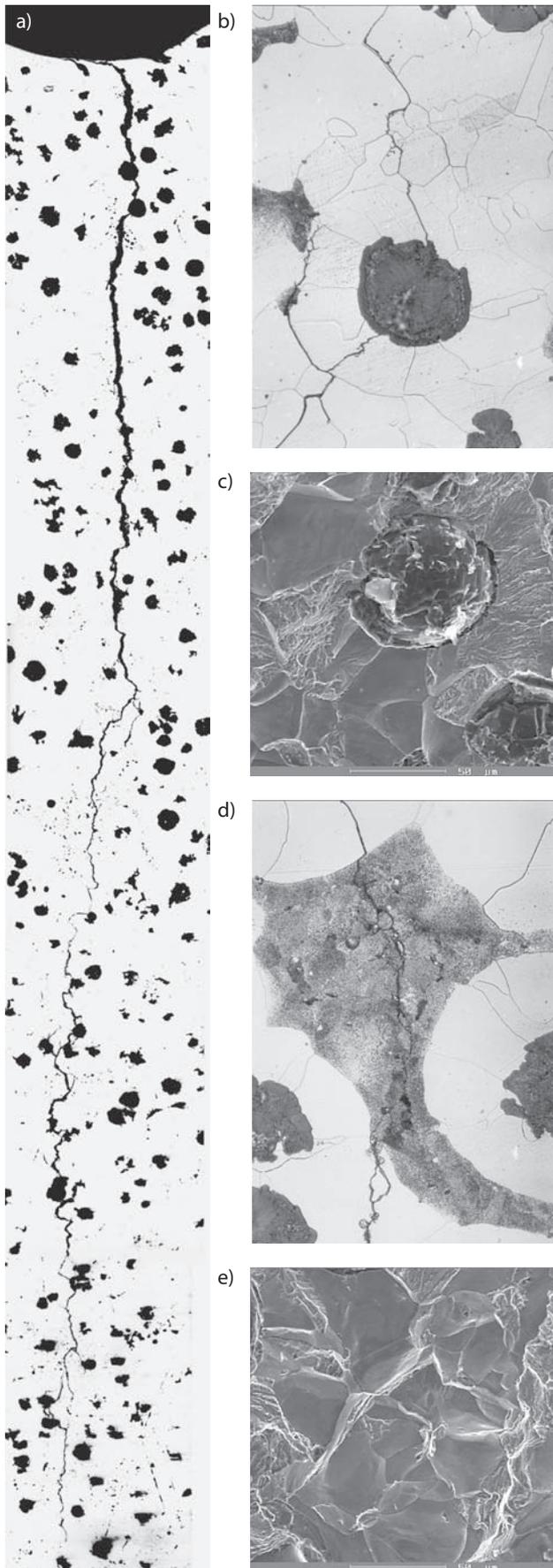

Figure 4 The fatigue life of nodular cast iron; the fatigue test using high frequencies [f = 20 kHz, T = 20 °C ± 10 °C, R = - 1]

Figure 5 Cast iron GJS-500-7: a) macro-structure of the fatigue crack, b) an inter- and transcrystalline cracks in the ferrite, c) an inter- and transcrystalline crack in the ferrite, a crack around the graphite precipitate d) transcrystalline cracking trough the pearlite, e) an intercrystalline crack in the ferrite
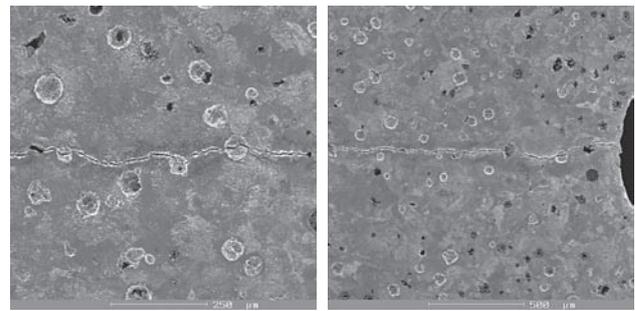
Figure 6 The fatigue crack trajectory: a, b) pearlitic-ferritic cast iron GJS-600-3.
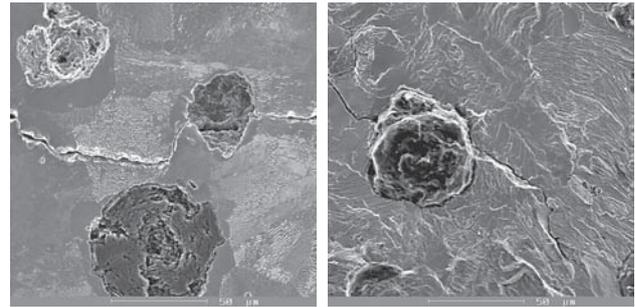
Figure 7 Cast iron GJS-600-3: a) transcrystalline fatigue cracking through the pearlite and graphite, b) a secondary crack in the fatigue crack plane
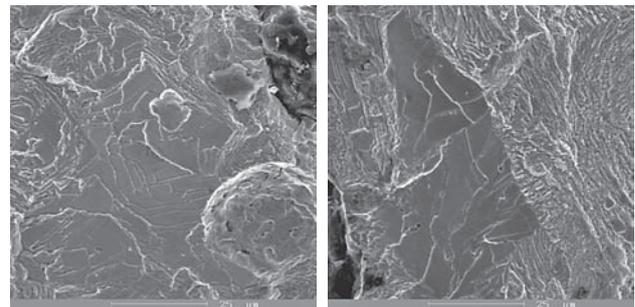
Figure 8 Cast iron GJS-600-3: a) crack propagation along the pearlite lamellas, b) a transcrystalline crack in the ferrite

greatest dispersion of the results occurred for the GJS-600-3 cast iron. The examination of the fatigue crack trajectory was made on a Neophot 32 optical microscope and a scanning microscope. Figure 5 represents the trajectory of propagation of a fatigue crack in ferritic-pearlitic cast iron after being loaded with high frequencies. The trajectory of the ferritic-pearlitic cast iron fatigue crack is shown in Figures 6÷8.

CONCLUSION

The results of fatigue testing of selected nodular cast iron grades for the conventional cycle limit of 10^7 have shown that with the decrease in the stress amplitude, σ_a, the number of cycles to fatigue failure increases. For the GJS-500-7 cast iron, the amplitude difference amounted to $\Delta\sigma_a = 96$ MPa; for the GJS-600-3 cast iron, $\Delta\sigma_a = 278$ MPa; and for the ADI cast iron, $\Delta\sigma_a = 15$ MPa. The

fractographic analysis of the fracture after testing within the upper and lower region of the cycle interval under examination ($N_f = 6 \times 10^6 \div 1,0 \times 10^{10}$ cycles) showed that the locations of crack initiation both on the specimen surface and under the specimen surface were casting defects and graphite particles. In the case of the ADI cast iron, we have the transcrystalline fracture mechanism, while for the GJS-600-3 cast iron at greater amplitudes, we observed also transcrystalline cracking, with intercrystalline cracking and brittle interlamellar cracking occurring in some places. With a low amplitude and a large number of cycles, the cracking exhibits a transcrystalline behaviour. In the case of the GJS-500-7 cast iron, a mixed fracture was observed within the entire examined interval of $6,0 \times 10^6 \div 1,0 \times 10^{10}$ cycles. In the GJS-500-7 and GJS-600-3 cast iron grades, numerous fatigue crack branches were observed, which were caused by the effect of the crack front with graphite particles and inhomogeneous structures, the increase in cracking at the matrix-graphite interface and the propagation of cracks through the graphite particles. In the process of fatigue crack initiation, non-metallic inclusions play an important role, particularly in the high-cycle area of loading [9,10].

REFERENCES

[1] F. Novy, O. Bokuvka, P. Palcek, M. Chalupova, Proceedings, 12th International Conference on mechanical behavior of materials, Como, Italy 2011, Effect of inclusions on very high cycle behaviour in a ferritic corrosion resisting steel, pp. 1408-1413, DOI: 10.1016/j.proeng.2011.04.234

[2] I. Marines, X. Bin, C. Bathias, An understanding of very high cycle fatigue of metals. Int. J. Fatigue 25 (2003), 1101–1107, DOI: 10.1016/S0142-1123(03)00147-6.

[3] J. Belan, High frequency fatigue test of in 718 alloy – microstructure and fractography evaluation, Metalurgija 54 (2015) 1, 59-62.

[4] F. Novy, M. Cincala, P. Kopas, O. Bokuvka, Mechanisms of high-strength structural materials fatigue failure in ultra-wide life region, Materials Science and Engineering A-Structural Materials Properties Microstructure and Processing 462 (2007), 189-192, DOI: 10.1016/j.msea.2006.03.147

[5] A. Vasko, L. Trsko, R. Konecna, Fatiuge behaviour of syntetic nodular cast irons, Metalurgija 54 (2015) 1, 19-22.

[6] R. Ulewicz, M. Mazur, Fatigue Testing Structural Steel as a Factor of Safety of Technical Facilities Maintenance, Production Engineering Archives (2013) 1, 32-34.

[7] O. Bokuvka, G. Nicoleto, M. Guagliano, L. Kunz, F. Novy, M. Chalupova, Fatigue of Materials at Low and High Frequency Loading, EDIS, Zilina, 2014, pp. 8-16 and 56-59.

[8] K. Salama, R.K. Lamerand, Proceedings, Conference Transactions of the Metallurgical Society of AIME, New York, 1982, Ultrasonic Fatigue, pp.109-118.

[9] T. Lipinski, A. Wach, The effect of fine non-metallic inclusions on the fatigue strength of structural steel, Archives of Metallurgy and Materials 60 (2015), 65-69, DOI: 10.1515/amm-2015-0010.

[10] M. Bursak, O. Bokuvka, Influence of technological Factors on Fatigue Properties of Steel sheets. Communications-Scientific letters of the University of Zilina, 8 (2006) 4, 34-37.